Journal of Civil and Hydraulic Engineering
https://www.acadlore.com/journals/JCHE

Seismic Safety Analysis of Asphalt Concrete Face Rockfill Dam on Thick Overburden Layer

Kai Peng[1], Xin Cheng[2], Weijun Cen[2*], Jialin Zhang[1]

[1] PowerChina Zhongnan Engineering Co., Ltd., 410014 Changsha, China
[2] College of Water Conservancy and Hydropower Engineering, Hohai University, 210098 Nanjing, China

* Correspondence: Weijun Cen (hhucwj@163.com)

Received: 10-26-2025 **Revised:** 12-12-2025 **Accepted:** 12-20-2025

Citation: K, Peng, X. Cheng, W. J. Cen, and J. L. Zhang, "Seismic safety analysis of asphalt concrete face rockfill dam on thick overburden layer," *J. Civ. Hydraul. Eng.*, vol. 4, no. 1, pp. 1–10, 2026. https://doi.org/10.56578/jche040101.

Abstract: A three-dimensional seismic response analysis of an asphalt concrete face rockfill dam constructed on a thick overburden layer at the upper reservoir of a pumped-storage power station was conducted using the nonlinear finite element method. The study focused on evaluating the seismic safety of the dam body and the seepage control system. The results indicated that, under the design seismic load, the peak dynamic displacements of the dam body in the horizontal, vertical, and axial directions were 23.87 cm, 10.44 cm, and 26.13 cm, respectively, and the peak accelerations were 2.98 m/s^2, 2.01 m/s^2, and 2.98 m/s^2, respectively. The maximum permanent deformations in the same directions were 18.42 cm, -61.60 cm, and -5.61 cm/18.69 cm, with a settlement ratio of 0.37%. For the asphalt concrete face slab, the peak dynamic displacements in the horizontal, vertical, and axial directions were 23.87 cm, 9.42 cm, and 24.86 cm, respectively. The maximum and minimum principal strains of the face slab after the earthquake were 1.29% and -0.74%. The maximum principal tensile strains of the geomembrane at the reservoir bottom during and after the earthquake were -1.43% and -1.50%. Under the seismic check conditions, the dynamic responses of the dam body, face slab, and geomembrane increased. Comprehensive analysis of the results shows that the seismic response patterns of the dam are consistent with the general characteristics of rockfill dams on thick overburden layers. The dynamic response of the asphalt concrete face slab around the reservoir and the geomembrane at the reservoir bottom did not exceed their respective safety thresholds, indicating that the dam exhibits high seismic safety under seismic loading.

Keywords: Thick overburden layer; Asphalt concrete face rockfill dam; Dynamic response; Seismic safety; Pumped-storage power station

1 Introduction

As an important component of power systems, pumped-storage power stations play a key role in peak shaving, frequency regulation, phase modulation, and emergency backup. Therefore, under the background of the "dual carbon" plan, the construction of pumped-storage power stations in China has made great progress during the "14th Five-Year Plan" period, ranking first in the world in both quantity and scale. Asphalt concrete face rockfill dams have the advantages of fast construction speed, strong adaptability to deformation, and high safety, making them particularly suitable for dam construction on thick overburden layers. In recent years, they have been widely used in the reservoirs of pumped-storage power station projects. For dam construction on overburden layers, there may be issues such as insufficient bearing capacity, difficulty in seepage control, and seismic liquefaction, and corresponding treatment of the foundation is generally required to meet engineering safety requirements [1]. For weak thick overburden layers, vibro-compacted gravel piles are commonly used foundation treatment methods. The composite foundation formed by the replacement and compaction of gravel piles can effectively improve the bearing capacity of the foundation.

At present, domestic and foreign scholars have conducted relevant research on the effectiveness of composite foundation treatment and the safety of asphalt concrete face rockfill dams. Xing et al. [2] used the nonlinear finite element method to calculate and analyze the effects of dam foundation treatment schemes such as consolidation grouting and jet grouting piles on the deformation of the dam body and the seepage body joints. Wang et al. [3]

obtained the shear strength of gravel pile composite foundations through laboratory shear model tests. Ruan et al. [4] conducted three-dimensional numerical simulations on gravel pile reinforced liquefiable silt foundations to explore the impact of gravel piles on the liquefaction resistance of foundations. Zhang and Zhang [5] used the elastoplastic damage interface element to numerically analyze the concrete face rockfill dam, which can trace the separation and re-contact between the face slab and the cushion at the interface. Tajdini et al. [6] adopted a small-scale shear strength test and concluded that the shear strength parameters increased with the increase of density and normal stress level. Gao et al. [7] proposed and investigated the improvement methods that reduce the high shear stress and high tensile stress of ultra-high asphalt concrete core based on the definition of stress level and the transmission mechanism of arch structures. Xu et al. [8] calculated and analyzed the impact of combined near-fault seismic motions and oblique incidence on the acceleration and stress of asphalt concrete face slabs, and the results showed that the tensile stress of the face slabs increased with the increase of the incident angle of P and SV waves. Cen et al. [9] used a three-dimensional nonlinear finite element method to calculate and analyze the dynamic response of a 135-meter-high concrete face rockfill dam on an overburden layer, comprehensively analyzing the dam's ultimate seismic capacity from multiple perspectives. Peng et al. [10] used a nonlinear dynamic elastoplastic method to calculate and analyze the seismic response of high face rockfill dams on overburden layers, and the results showed that there is a critical overburden layer thickness, which causes the acceleration amplification factor of the site to have a maximum value. Wang et al. [11] used an improved equivalent viscoelastic model to calculate and analyze the seismic response of a 161-meter-high asphalt concrete face rockfill dam. The results showed that the maximum tensile strain of the face slab was less than the general allowable value, and the dam had good seismic safety. Li et al. [12] used an elastoplastic constitutive model to study the dynamic response of face rockfill dams of different heights on the same thick overburden layer under long-period seismic motion. Wang et al. [13] used a three-dimensional nonlinear finite element method to conduct static and dynamic calculations and analysis on a 161-meter-high asphalt face rockfill dam in a strong earthquake zone, and the results showed that the overall safety performance of the dam was good, and there would be no major safety problems during earthquakes. Albano et al. [14] studied the seismic performance of high asphalt concrete face rockfill dams in strong earthquake zones. Wang et al. [15] considered the spatial arbitrariness of the azimuth angle and oblique incidence angle of P-wave, established the wave input method of oblique incidence of P-wave in three dimensions, and established an empirical formula of instantaneous tensile strength of asphalt concrete varying with strain rate on the basis of the test results. Song et al. [16] considered the spatial variability and correlation of covering material parameters and proposed a new non-destructive stochastic finite element calculation method to study the influence of randomness of static and dynamic parameters on the seismic response of asphalt concrete core dam. Sun et al. [17] analyzed the seismic vulnerability of high asphalt concrete core rockfill dam and concluded that GMs with longer duration has higher relative settlement ratio, stress demand capacity ratio and exceeding probability than GMs with shorter duration. Ma et al. [18] used orthogonal test method to analyze the sensitivity of an asphalt concrete slab, the results show that the sensitivity of initial bulk modulus base Kb, damage ratio Rf and initial elastic modulus base K is relatively high, which has a significant impact on the calculation results. Li et al. [19] derived the free-field formula for SV waves at any incident angle and established an oblique incident input model for SV waves, analyzing the impact of the incident angle on the seismic response of asphalt concrete face slabs from both stress and acceleration perspectives.

This paper takes the asphalt concrete face dam on the thick overburden layer at the upper reservoir of a pumped-storage power station as the research object. The three-dimensional nonlinear finite element method is used to calculate and analyze the dynamic response of the dam under design seismic and check seismic conditions, and the seismic safety of the dam is evaluated. The calculation results provide guidance for similar engineering design, construction, and safe operation.

2 Project Overview

A pumped-storage power station consists of key structures such as an upper reservoir, a lower reservoir, a water conveyance system, and a powerhouse. The lithology of the upper reservoir is relatively complex, with significant overburden thickness and poor homogeneity at the dam body and basin bottom, influenced by limestone dissolution and subsequent collapse accumulation. The overburden thickness ranges from 13.4 m to 110.4 m, with an average thickness of 47.6 m. Based on the analysis of the bearing capacity of the natural overburden foundation, it is proposed to use vibro-compacted gravel piles for reinforcement in specific areas of the overburden layer. The treatment range is defined as extending 20 m upstream and 35 m downstream from the anti-seepage connection plate at the bottom of the reservoir, with a treatment depth of 30 m. The overburden layer treated with vibro-compacted gravel piles can be regarded as a composite foundation. The upper reservoir dam is an asphalt concrete face rockfill dam, with a maximum dam height of 36 m, a crest elevation of 651 m, and a crest width of 10.00 m. The normal water level is 646.00 m. Figure 1 shows the typical cross-section of the dam.

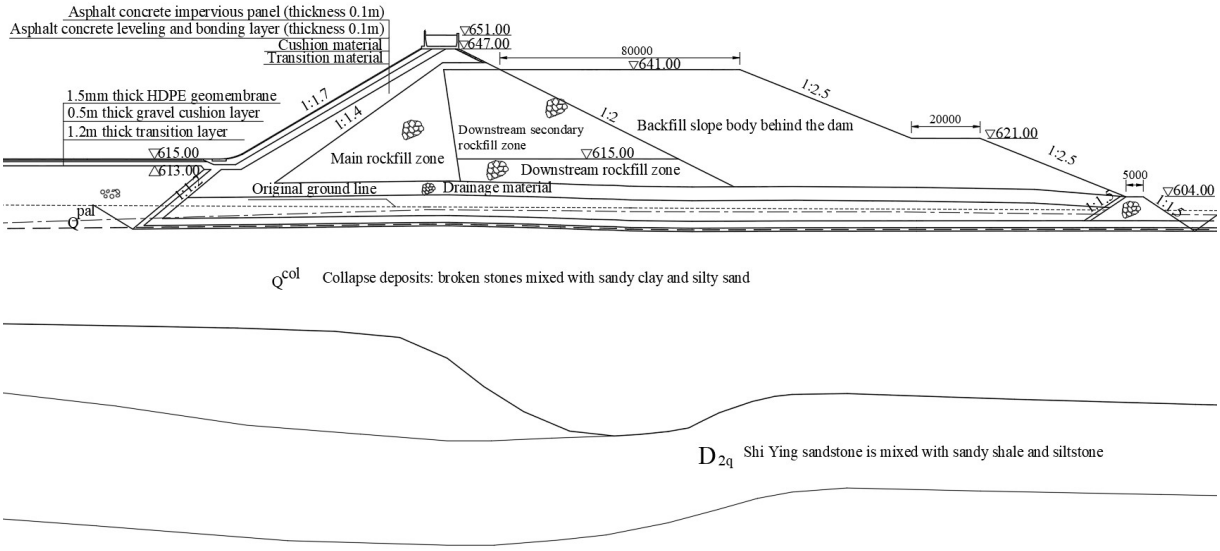

Figure 1. Typical cross-section of the dam

3 Dynamic Constitutive Model for Earth and Rock Materials

In dynamic calculations, the earth and rock materials of the dam body are regarded as viscoelastic materials, and the equivalent shear modulus G and equivalent damping ratio are used to reflect the nonlinearity and hysteresis of their dynamic stress-strain relationship. These relationships are expressed as functions of the shear modulus and damping ratio in relation to the dynamic shear strain. This study adopts the improved Hardin-Drnevich model by scholar Zhujiang Shen to calculate the dynamic modulus and damping ratio of rockfill material, which is expressed as:

$$\text{Dynamic Modulus } G_d = k_2/\left(1 + k_1\gamma_d\right) P_a \left(\sigma_m/P\right)^n \tag{1}$$

$$\text{Damping Ratio } \lambda = \lambda_{\max} k_1\bar{\gamma}_d/\left(1 + k_1\bar{\gamma}_d\right) \tag{2}$$

$$\text{Maximum Shear Modulus } G_{\max} = K_2 P_a \left(\sigma'_m/P_a\right)^n \tag{3}$$

where, γ_d is the dynamic shear strain; σ_m is the mean effective stress; p_a is the atmospheric pressure; K_1, K_2, and n are experimental parameters.

The equivalent nodal force method is used to calculate the earthquake permanent deformation of the earth-rock dam. The residual volumetric strain and residual shear strain obtained by dynamic calculation are converted into six strain components in rectangular coordinate system according to certain assumptions. These are then used to compute the "equivalent nodal forces", which are applied to the dam body for a static calculation to obtain the earthquake permanent deformation of the earth-rock dam.

The residual volumetric strain and shear strain calculations use the model proposed by Zhujiang Shen, with their incremental forms as follows:

$$\Delta\varepsilon_{vr} = c_1 \left(\gamma_d\right)^{c_2} \exp\left(-c_3 S_l^2\right) \Delta N/(1 + N) \tag{4}$$

$$\Delta\gamma_r = c_4 \left(\gamma_d\right)^{c_5} S_l^2 \Delta N/(1 + N) \tag{5}$$

where, $\Delta\varepsilon_{vr}$ is the residual volumetric strain; $\Delta\gamma_r$ is the residual shear strain; S_l is the shear stress level; N and ΔN are the vibration number and its increment, respectively; c_1, c_2, c_3, c_4, c_5 are experimental parameters determined by conventional dynamic triaxial liquefaction tests.

4 Calculation Model and Conditions

4.1 Finite Element Model

Based on the layout plan and sectional drawings of the upper reservoir hub, a three-dimensional finite element model of the "reservoir-dam" system was established, with the bottom boundary of the model set as the bedrock.

Figure 2 shows the overall finite element mesh of the "reservoir-dam" system, where the mesh has been divided into hexahedral elements, supplemented locally by pentahedral and tetrahedral elements. Contact elements are set between the face slab and the cushion layer around the reservoir, as well as between the geomembrane and the cushion layer at the reservoir bottom, to simulate their contact behavior. The overall dam mesh consists of 71,719 nodes and 70,979 elements, including 4,672 asphalt concrete face slab elements and 2,478 geomembrane elements.

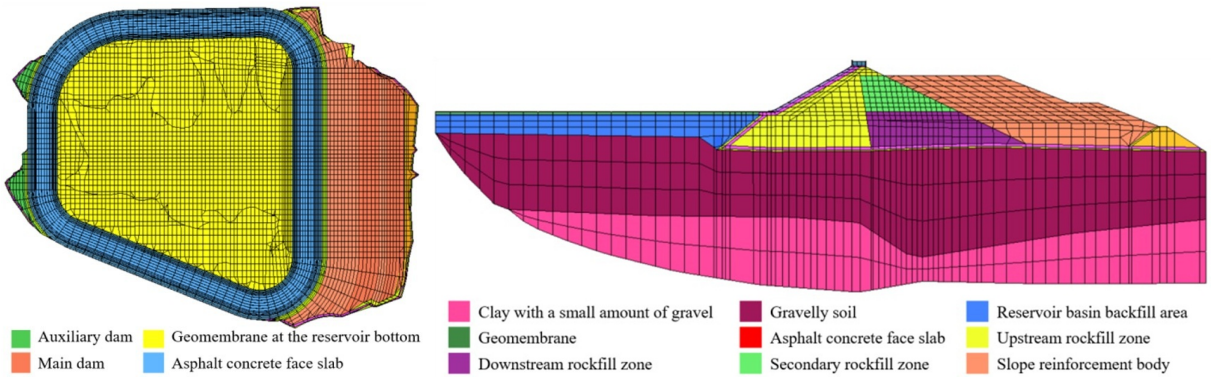

(a) Overall dam and basin (b) Typical cross-section of the riverbed section

Figure 2. Overall finite element mesh of the upper reservoir "reservoir-dam" system and typical cross-section

4.2 Dynamic Calculation Parameters

The overburden layer locally treated with vibro-compacted gravel piles is regarded as a composite foundation. A three-dimensional static calculation of the dam was performed first, and the resulting stress field was used as the initial condition for the dynamic calculation. The dynamic calculation adopted the equivalent viscoelastic dynamic constitutive model, and the seismic permanent deformation was calculated using the Zhujiang Shen permanent deformation model [20]. Based on the results of large-scale indoor triaxial static tests, and considering the lithology, strength indices, and relevant physical and mechanical properties of the dam materials in this project, as well as drawing comparisons with other projects like the Wuhai Pumped-Storage Power Station and Maqin Pumped-Storage Power Station concrete face rockfill dams, while referencing the mechanical characteristics of deep overburden layers at the Lawa Hydropower Station, and combining with engineering calculation experience, the suitable Hardin-Drnevich dynamic constitutive model and permanent deformation parameters attained by Zhujiang Shen for the upper reservoir dam materials and overburden layer were determined, as shown in Table 1.

Table 1. Dynamic calculation parameters for main dam materials

Zone	K_2	n	λ_{max}	c_1	c_2	c_3	c_4	c_5
Asphalt concrete face slab	1200	0.23	0.10	1	1	/	0.015	1.0
Cushion layer	2278	0.39	0.20	0.0042	0.66	1	0.0764	0.85
Transition layer	2463	0.39	0.19	0.0038	0.64	1	0.0736	0.90
Main rockfill zone	1929	0.39	0.19	0.0046	0.68	1	0.0782	0.82
Downstream rockfill zone	1162	0.42	0.22	0.0053	0.73	1	0.0865	0.70
Downstream secondary rockfill zone	1052	0.50	0.25	0.0110	1.00	1	0.1100	0.50
Composite foundation	566	0.61	0.27	0.0047	0.81	/	0.1300	1.26

4.3 Seismic Input

The corresponding basic seismic intensity for the dam site area is VI degree, and the design intensity is VII degree. The characteristic period of the basic seismic acceleration response spectrum for class II site is 0.35s. According to the *Code for Seismic Design of Hydraulic Structures of Hydropower Project* (NB 35047-2015) [21] and the principles for determining major engineering response spectra, the upper reservoir dam is classified as a Grade 1 water retention structure with Category A seismic fortification. The three-dimensional finite element dynamic calculation uses artificial synthesized seismic waves provided by the seismic hazard assessment department, based on the standard rock spectrum. The acceleration time-history curve for a 100-year exceedance probability of 2% earthquake (design earthquake) is used as the basic dynamic condition, and the acceleration time-history curve for a 100-year exceedance probability of 1% earthquake (check earthquake) is used for dynamic verification. The

corresponding peak horizontal accelerations are 117.0 cm/s^2 and 142.0 cm/s^2, respectively. Figure 3 shows the acceleration time-history curve of the design earthquake at the dam site. In dynamic calculations, the vertical acceleration is taken as two-thirds of the peak horizontal acceleration.

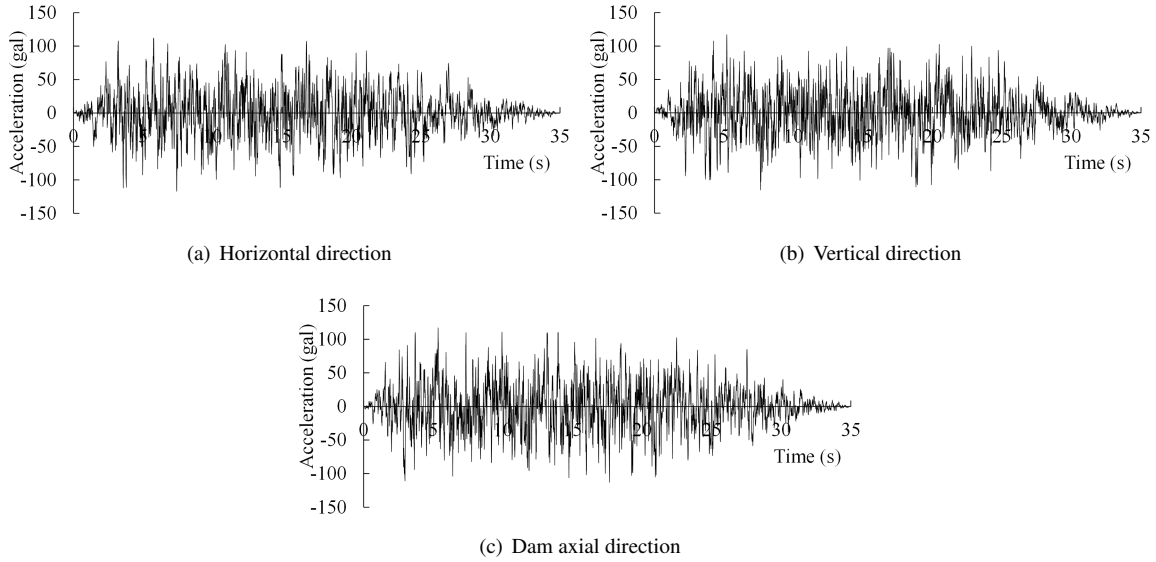

(a) Horizontal direction

(b) Vertical direction

(c) Dam axial direction

Figure 3. Acceleration time-history curves of the design earthquake on bedrock

5 Seismic Safety Analysis of the Dam Body

During an earthquake, the dynamic displacement of the dam generally exhibits a gradual increase from the bottom of the overburden layer to the dam crest. Due to the deep and relatively weak overburden layer of the dam foundation, the dynamic displacement response at the dam crest remains significant even under moderate seismic conditions (design intensity VII degree). Figure 4 presents the dynamic displacement envelope diagram of a typical dam cross-section under the design earthquake (100-year exceedance probability of 2%, the same hereafter). Under the design earthquake, the peak dynamic displacements of the dam in the horizontal, vertical, and axial directions are 23.87 cm, 10.44 cm, and 26.13 cm, respectively. Under the check earthquake, the peak dynamic displacements of the dam in the horizontal, vertical, and axial directions are 31.24 cm, 16.27 cm, and 37.14 cm, respectively. Compared to the design earthquake, the dynamic displacement response of the dam under the check earthquake increases, with the peak dynamic displacements generally being larger.

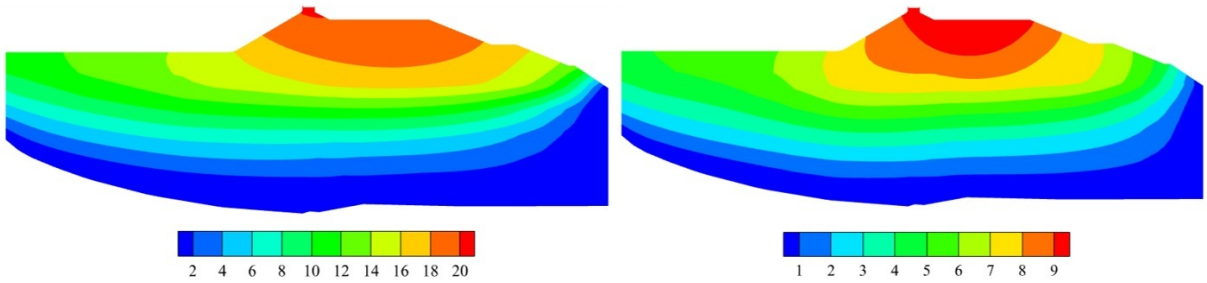

(a) Horizontal direction

(b) Vertical direction

Figure 4. Dynamic displacement envelope diagram of a typical dam cross-section under design earthquake (Unit: cm)

The acceleration response of the dam generally shows a gradual increase from the bottom of the overburden layer to the dam crest, with the most intense response near the dam crest. Figure 5 shows the acceleration envelope diagram of a typical dam cross-section under the design earthquake. Under the design earthquake, the peak accelerations of the dam in the horizontal, vertical, and axial directions are 2.98 m/s^2, 2.01 m/s^2, and 2.98 m/s^2, respectively, with corresponding amplification factors of 2.55, 2.58, and 2.55. Under the check earthquake, the peak accelerations of the dam in the horizontal, vertical, and axial directions are 3.42 m/s^2, 2.29 m/s^2, and 3.42 m/s^2, respectively, with

corresponding amplification factors of 2.41, 2.42, and 2.41. Compared to the design earthquake, the acceleration response of the dam under the check earthquake increases, but the acceleration amplification factors decrease, which is consistent with the general pattern.

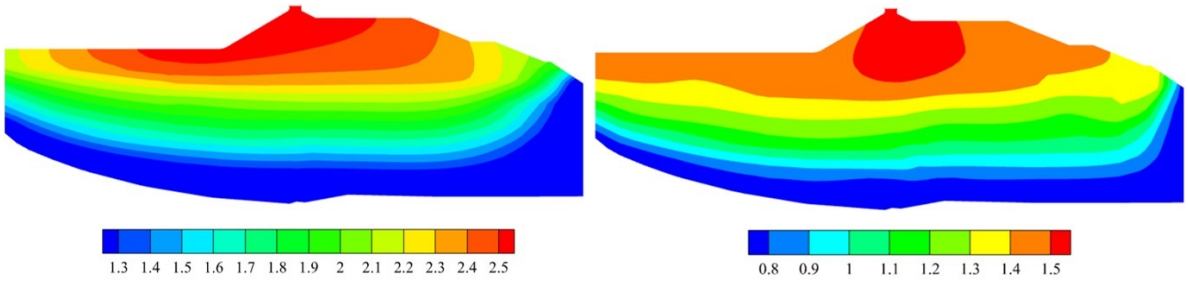

(a) Horizontal direction (b) Vertical direction

Figure 5. Acceleration envelope diagram of a typical dam cross-section under design earthquake (Unit: m/s^2)

Figure 6 presents the permanent deformation cloud diagram of the dam under the design earthquake. Due to the water pressure, the post-earthquake permanent deformation of the dam body in the horizontal direction is mainly downstream, while the self-weight causes the post-earthquake vertical permanent deformation to manifest as subsidence, with the extremum located near the dam crest. Under the design earthquake, the peak permanent deformations of the dam in the horizontal, vertical, and axial directions are 18.42 cm, -61.60 cm, and -5.61 cm/18.69 cm, respectively, with a settlement rate of 0.37%. Under the check earthquake, the peak permanent deformations of the dam in the horizontal, vertical, and axial directions are 22.28 cm, -71.62 cm, and -8.13 cm/23.02 cm, respectively, with a settlement rate of 0.43%. Compared to the design earthquake, the permanent deformation of the dam under the check earthquake increases, which is consistent with the general pattern. Due to the weak and deep overburden layer in this project, the settlement rate of the dam (including the foundation) is higher than that of rockfill dams of the same height on bedrock or on harder overburden layers but does not exceed the general settlement rate limit of 0.6 to 0.8% controlled by engineering design.

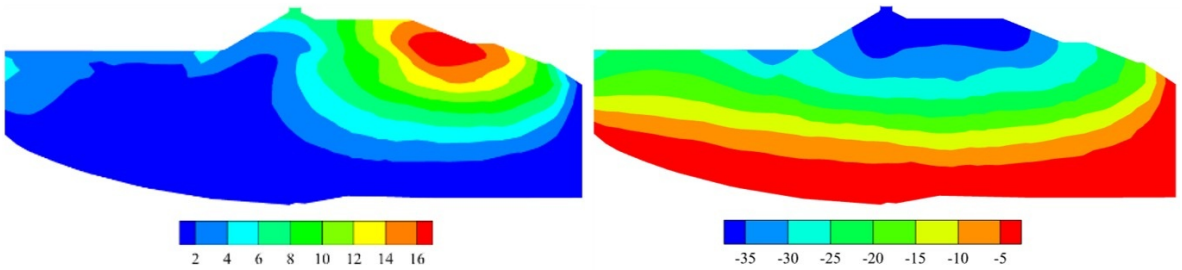

(a) Horizontal direction deformation (b) Seismic subsidence

Figure 6. Permanent deformation cloud diagram of dam under design earthquake (Unit: cm)

6 Seismic Safety Analysis of the Seepage Control System

6.1 Seismic Response of the Asphalt Concrete Face Slab

Figure 7 presents the dynamic displacement envelope value of asphalt concrete slab under design earthquake. It can be seen from the figure that the dynamic displacement response of asphalt concrete face slab under earthquake mainly concentrates on some face slabs of dam body, and its value basically increases from dam foundation to dam top, reaching the maximum near the top of face slab; The dynamic displacement response of some slabs on the bank slope of the reservoir is very small, which accords with the general law of seismic response of slabs in the "reservoir-dam" project of pumped storage power station. Under the design earthquake, the extreme values of the dynamic displacement of asphalt concrete slabs along the river, vertically and axially are 23.87 cm, 9.42 cm and 24.86 cm, respectively. Under the check earthquake, the extreme values of the dynamic displacement of asphalt concrete slabs along the river, vertically and axially are 30.10 cm, 13.16 cm and 36.87 cm, respectively. Compared with the design earthquake, the dynamic displacement of the slab under the check earthquake has increased.

Figure 8 shows the principal tensile strain envelope diagram of the asphalt concrete face slab under the design earthquake. Under the design earthquake, the maximum dynamic principal compressive strain and principal tensile

strain of the asphalt concrete face slab are 0.81% and -0.57%, respectively. After superimposing static and dynamic effects, the maximum and minimum principal strains of the slab are 0.93% and -0.66%, respectively, while the maximum and minimum principal strains after the earthquake are 1.29% and -0.74%. Under the check earthquake, the maximum dynamic principal compressive strain and principal tensile strain of the slab are 0.96% (compressive) and -0.77% (tensile), respectively. After superimposing static and dynamic effects, the maximum and minimum principal strains of the slab are 1.11% and -0.84%, respectively, and the maximum and minimum principal strains after the earthquake are 1.59% and -0.95%. Compared to the design earthquake, the principal strains of the slab increase under the check earthquake, consistent with the general pattern. The maximum principal compressive and tensile strains under different conditions are below the allowable values of 3.0% for compressive strain and 1.0% for tensile strain of asphalt concrete; therefore, the asphalt concrete face slab is safe during and after the earthquake [22].

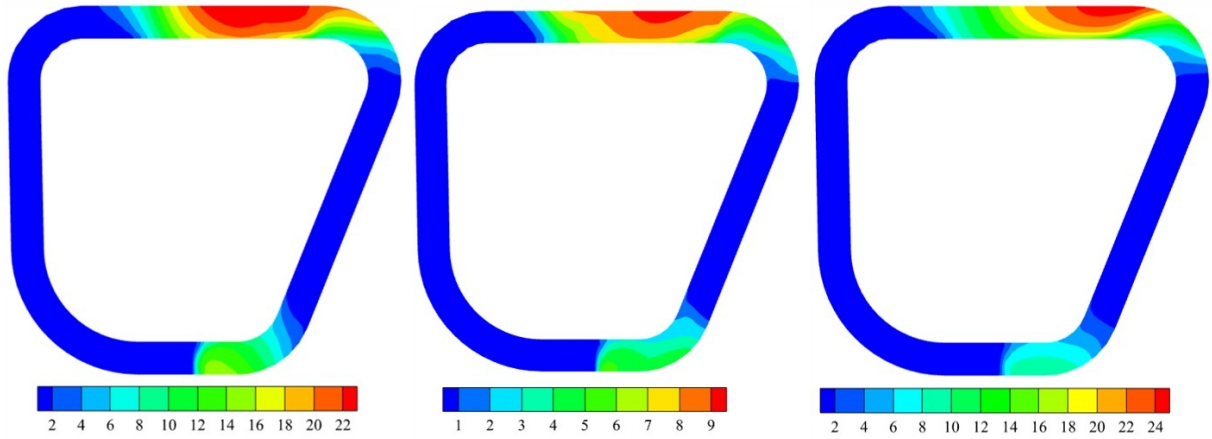

(a) Horizontal direction (b) Vertical direction (c) Dam axial direction

Figure 7. Dynamic displacement envelope diagram of the face slab under design earthquake (Unit: cm)

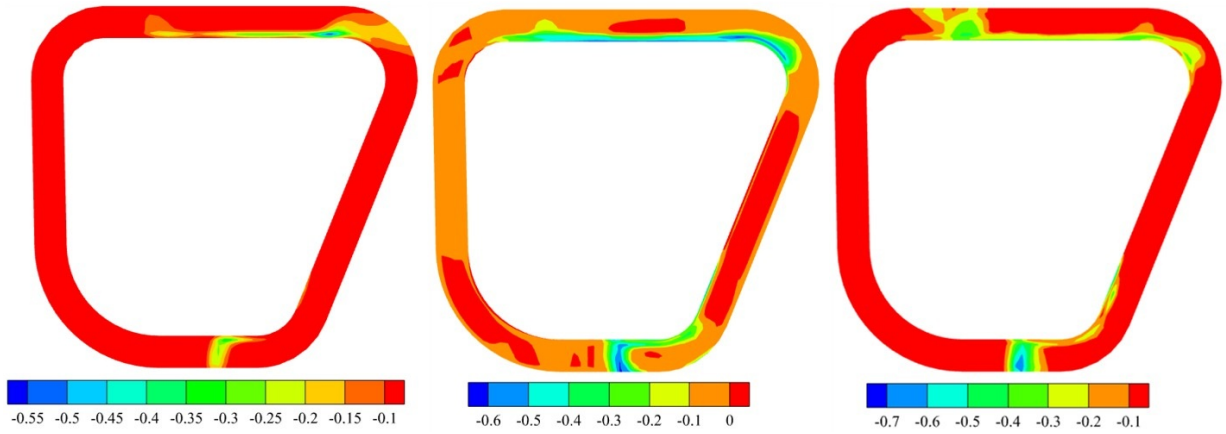

(a) Dynamic principal tensile strain (b) "Static + dynamic" principal tensile strain (c) Post-earthquake principal tensile strain

Figure 8. Principal tensile strain envelope diagram of the face slab under design earthquake (Unit: %)

6.2 Seismic Response of the Geomembrane at the Reservoir Bottom

Figure 9 shows the principal tensile strain envelope diagram of the geomembrane at the reservoir bottom under the design earthquake. Under the design earthquake, the maximum dynamic principal tensile strain of the geomembrane at the reservoir bottom is -0.28%, the maximum principal tensile strain after superimposing static and dynamic effects is -1.43%, and the maximum post-earthquake principal tensile strain is -1.50%. Under the check earthquake, the maximum dynamic principal tensile strain of the geomembrane is -0.36%, the maximum principal tensile strain after superimposing static and dynamic effects is -1.62%, and the maximum post-earthquake principal tensile strain is -1.98%. The maximum principal tensile strain areas are located near the boundary between the rock and the

overburden layer at the reservoir bottom, and the maximum strain values are below the tensile strain threshold of 2.5% for the geomembrane, satisfying the seismic safety requirements.

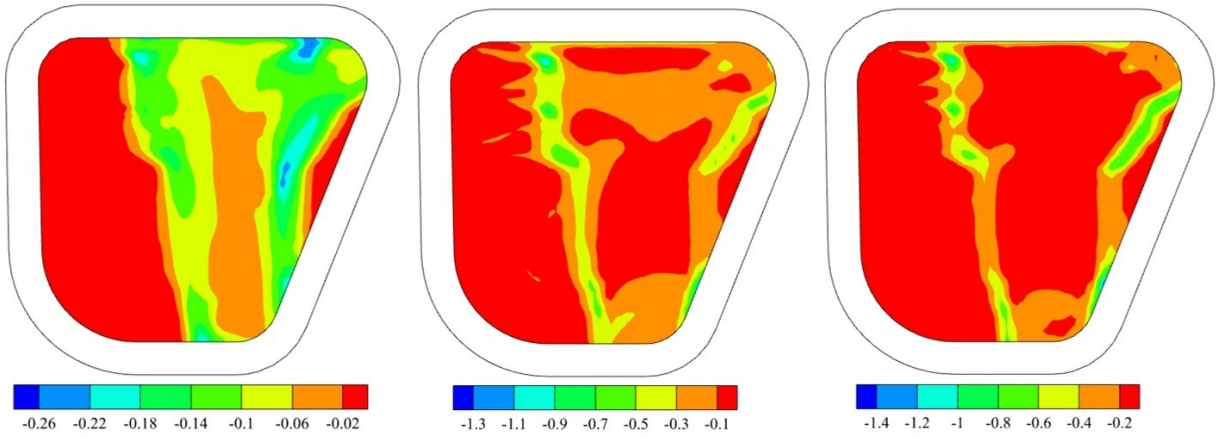

(a) Dynamic principal tensile strain (b) "Static + dynamic" principal tensile strain (c) Post-earthquake principal tensile strain

Figure 9. Principal tensile strain envelope diagram of the face slab under design earthquake (Unit: %)

7 Conclusions

This study conducted a three-dimensional dynamic finite element calculation for an asphalt concrete face rockfill dam on a thick overburden layer at the upper reservoir of a pumped-storage power station, analyzing the dynamic response of the dam body and seepage control system under both design and check earthquakes. The main conclusions are as follows:

(1) Under seismic action, the distribution of dynamic displacement, acceleration, and permanent deformation of the dam body is reasonable. The peak values increase with the increase of seismic input values. Under the design earthquake, the peak dynamic displacements of the dam in the horizontal, vertical, and axial directions are 23.87 cm, 10.44 cm, and 26.13 cm, respectively; the peak accelerations are 2.98 m/s^2, 2.01 m/s^2, and 2.98 m/s^2, with corresponding amplification factors of 2.55, 2.58, and 2.55; the peak permanent deformations are 18.42 cm, -61.60 cm, and -5.61 cm/18.69 cm, with a settlement rate of 0.37%. Under the check earthquake, the distribution pattern of the above dynamic response quantities is similar to that under the design earthquake, but the peak values increase. Since the dam is built on a weak and deep overburden layer, the settlement rate of the dam (including the foundation) is higher than that of rockfill dams of the same height on bedrock or harder overburden layers, but is less than the engineering design control limit value of 0.6 to 0.8%.

(2) Under the design earthquake, the peak dynamic displacements of the asphalt concrete face slab in the horizontal, vertical, and dam axial directions are 23.87 cm, 9.42 cm, and 24.86 cm, respectively; the maximum and minimum principal strains after superimposing static and dynamic effects are 0.93% and -0.66%, respectively; the maximum and minimum principal strains after the earthquake are 1.29% and -0.74%, respectively. Under the check earthquake, the above dynamic response quantities increase, but the peak principal compressive and tensile strains of the face slab are below the allowable compressive and tensile strain values of asphalt concrete. Therefore, the asphalt concrete face slab will not undergo compressive or tensile failure during and after the earthquake, meeting the seismic safety operation requirements.

(3) Under the design earthquake, the maximum principal tensile strains of the geomembrane at the reservoir bottom during and after the earthquake are -1.43% and -1.50%, respectively. Under the check earthquake, the maximum principal tensile strains during and after the earthquake increase to -1.62% and -1.98%, which are below the tensile strain threshold of 2.5% for the geomembrane, satisfying the seismic safety operation requirements. For safety considerations, it is suggested to minimize or control the deformation differences of the geomembrane in the excavation and backfill areas near the reservoir bottom during design and construction to avoid the possibility of local tensile failure of the geomembrane.

Comprehensive analysis of the dam's seismic response indicates that the dam's seismic response law aligns with the general characteristics of rockfill dams on thick overburden layers. Compared to the design earthquake, the dynamic response quantities of the dam body and seepage control system under the check earthquake increase, but the dynamic responses of the asphalt concrete face slab around the reservoir and the geomembrane at the reservoir bottom do not exceed their respective safety thresholds, indicating high seismic safety of the dam under seismic action.

Author Contributions

Conceptualization, K.P. and W.C.; methodology, K.P.; software, X.C.; validation, K.P., X.C., W.J.C., and J.L.Z.; formal analysis, K.P.; investigation, X.C.; resources, X.C.; data curation, W.J.C.; writing—original draft preparation, X.C.; writing—review and editing, W.J.C.; visualization, X.C.; supervision, K.P.; project administration, W.J.C.; funding acquisition, W.J.C. All authors have read and agreed to the published version of the manuscript.

Data Availability

The data used to support the findings of this study are available from the corresponding author upon request.

Conflicts of Interest

The authors declare that they have no conflicts of interest.

References

[1] J. L. Bi, "Seepage analysis method and application of gravel pile composite foundation for earth-rock dams on deep overburden layers," Master thesis, Nanjing: Hohai University, 2014.

[2] J. Y. Xing, Z. C. Guan, and X. L. Lv, "Overburden treatment for concrete face rockfill dams and its application in hekoucun project," *Chin. J. Geotech. Eng.*, vol. 42, no. 7, pp. 1368–1376, 2020. https://doi.org/10.11779/CJGE202007021

[3] J. H. Wang, J. W. Jiang, Y. F. Sun, B. T. Wang, S. Y. Han, J. Y. Zuo, and Y. Tang, "Physical model test study on strength characteristics of gravel pile composite foundation," *Int. J. Phys. Model. Geotech.*, vol. 24, no. 6, pp. 286–297, 2024. https://doi.org/10.1680/jphmg.23.00046

[4] D. H. Ruan, Y. M. Zhang, Z. Wang, and C. X. Huang, "The numerical analysis of gravel pile reinforcing liquefiable silt," *Appl. Mech. Mater.*, vol. 353, pp. 265–269, 2013. https://doi.org/10.4028/www.scientific.net/AMM.353-356.265

[5] G. Zhang and J. M. Zhang, "Numerical modeling of soil–structure interface of a concrete-faced rockfill dam," *Comput. Geotech.*, vol. 36, no. 5, pp. 762–772, 2009. https://doi.org/10.1016/j.compgeo.2009.01.002

[6] M. Tajdini, R. Mahinroosta, and H. Taherkhani, "An investigation on the mechanical properties of granular materials in interface with asphaltic concrete," *Constr. Build. Mater.*, vol. 62, pp. 85–95, 2014. https://doi.org/10.1016/j.conbuildmat.2014.03.016

[7] J. Gao, F. Dang, and Z. Ma, "Investigation for the key technologies of ultra-high asphalt concrete core rockfill dams," *Soils Found.*, vol. 59, no. 6, pp. 1740–1757, 2019. https://doi.org/10.1016/j.sandf.2019.07.013

[8] S. N. Xu, Z. Q. Song, and C. Li, "Seismic response of asphalt concrete face rockfill dam under combined oblique incidence of near-fault ground motions," *J. Water Resour. Water Eng.*, vol. 35, no. 4, pp. 127–135, 2024. https://doi.org/10.11705/j.issn.1672-643X.2024.04.15

[9] W. J. Cen, Z. Q. Zhang, T. Zhou, H. K. Yang, and P. C. Lu, "Maximum seismic capacity of a high concrete-face rockfill dam on alluvium deposit," *Adv. Sci. Technol. Water Resour.*, vol. 36, no. 2, pp. 1–5, 2016. https://doi.org/10.3880/j.issn.1006-7647.2016.02.001

[10] X. F. Peng, Y. L. Zhu, and C. Ma, "Analysis of the influence of overburden layer thickness on dynamic response of concrete face rockfill dam," *J. Hefei Univ. Technol. (Nat. Sci.)*, vol. 43, no. 1, pp. 98–102, 2020. https://doi.org/10.3969/j.issn.1003-5060.2020.01.017

[11] D. L. Wang, J. Tang, and H. Wang, "Seismic stability analysis of asphalt concrete face rockfill dam of pumped storage power station in strong earthquake area," *Water Resour. Power*, vol. 42, no. 1, pp. 102–105, 2024. https://doi.org/10.20040/j.cnki.1000-7709.2024.20230485

[12] H. M. Li, N. H. Zhai, M. D. Zhao, C. K. Chen, and L. Y. Wang, "Long-period seismic dynamic response of high face rockfill dam with deep overburden," *Water Resour. Power*, vol. 41, no. 8, pp. 109–112, 2023. https://doi.org/10.20040/j.cnki.1000-7709.2023.20221724

[13] H. Wang, W. J. Cen, D. L. Wang, and J. Tang, "Seismic safety of a high asphalt concrete-faced rockfill dam in strong earthquake area," *J. Water Resour. Water Eng.*, vol. 34, no. 5, pp. 165–171, 2023. https://doi.org/10.11705/j.issn.1672-643X.2023.05.19

[14] M. Albano, G. Modoni, P. Croce, and G. Russo, "Assessment of the seismic performance of a bituminous faced rockfill dam," *Soil Dyn. Earthq. Eng.*, vol. 75, pp. 183–198, 2015. https://doi.org/10.1016/j.soildyn.2015.04.005

[15] F. Wang, Z. Song, Y. Liu, and C. Li, "Response characteristics and tensile failure evaluation of asphalt concrete core wall under spatial oblique incidence of P-wave," *Eng. Struct.*, vol. 276, p. 115340, 2023. https://doi.org/10.1016/j.engstruct.2022.115340

[16] Z. Song, Z. Wang, B. Luo, F. Wang, S. N. Xu, and Y. Liu, "Seismic response of asphalt concrete core dam

considering spatial variability of overburden foundation materials," *Arab. J. Sci. Eng.*, vol. 47, no. 10, pp. 12 605–12 620, 2022. https://doi.org/10.1007/s13369-022-06567-1

[17] B. Sun, M. Deng, S. Zhang, C. Wang, and M. Du, "Seismic performance assessment of high asphalt concrete core rockfill dam considering shorter duration and longer duration," *Structures*, vol. 39, pp. 1204–1217, 2022. https://doi.org/10.1016/j.istruc.2022.03.040

[18] B. Ma, W. Zhang, Z. Shen, D. Zhou, H. Yao, and R. Wang, "Identification of sensitive parameters for deformation of asphalt concrete face rockfill dam of pumped storage power station," *Water*, vol. 14, no. 17, p. 2634, 2022. https://doi.org/10.3390/w14172634

[19] C. Li, Z. Song, F. Wang, and Y. Liu, "Analysis of the seismic response and failure evaluation of the slabs of asphalt concrete-faced rockfill dams under SV-Waves with arbitrary angles," *Comput. Geotech.*, vol. 168, p. 106125, 2024. https://doi.org/10.1016/j.compgeo.2024.106125

[20] W. J. Cen, *Seismic Calculation Theory and Application of Earth-Rock Dams: Constitutive Model · Fluid-Solid Coupling · Seismic Input*. Beijing: Science Press, 2022.

[21] National Energy Administration, "Seismic design code for hydraulic structures of hydropower projects: NB35047-2015," Beijing, 2015.

[22] National Energy Administration, "Design code for asphalt concrete face and core wall of earth-rock dams: NB/T11015-2022," Beijing, 2022.